Analysis of the Distance Dependence and Magnitude of the π_+, π_- and π_+^*, π_-^* Splittings in a Series of Diethynyl[n]staffanes: An ab Initio Molecular Orbital Study

Michael N. Paddon-Row*,† and Kenneth D. Jordan*,§

Contribution from the School of Chemistry, University of New South Wales, P.O. Box 1, Kensington, NSW, Australia 2033, and the Department of Chemistry, University of Pittsburgh, Pittsburgh, Pennsylvania 15260

Received October 13, 1992

Abstract: Through-bond orbital interactions between the π orbitals and between the π^* orbitals of the first five members of the series of α,ω-diethynyloligo[1.1.1]propellanes, or α,ω-diethynyl[n]staffanes, **4(1)**–**4(5)**, have been investigated using ab initio MO theory. The π_+,π_- and π_+^*,π_-^* splittings of **4(1)**–**4(5)** were obtained in the Koopmans' theorem approximation, using the STO-3G, 3-21G, and 6-31G* basis sets. For the first three members of the series, calculations were also performed with several other basis sets. It is found that the minimal STO-3G basis set failed to give satisfactory qualitative trends in the π_+,π_- and π_+^*,π_-^* splittings for **4(1)**–**4(5)**, whereas the 3-21G basis set is adequate in this regard. The π_+^*,π_-^* splittings (ΔE) of **4(1)**–**4(5)** followed a nearly exponential decay with increasing length of the staffane: $\Delta E = A \exp(-\beta m)$, where m refers to the number of C–C bonds in the relays connecting the acetylenic chromophores. On the other hand, the π_+,π_- splittings show a marked deviation from an exponential distance dependence. However, even in this case, the splittings "settle down" to a near-exponential distance dependence for the longer bridges. The average 3-21G β values are 0.24 per bond (for the π_+,π_- splittings) and 0.37 per bond (for the π_+^*,π_-^* splittings). These β values imply that the π_+,π_- and π_+^*,π_-^* splittings for **4(1)**–**4(5)** fall off surprisingly slowly with increasing bridge length. The distance dependence of the π_+,π_- and the π_+^*,π_-^* splittings for **4(1)**–**4(5)** is even weaker than that calculated for the polynorbornyl dienes, **3(2)**–**3(6)**, for which the average 3-21G β values are 0.39 (π_+,π_-) and 0.54 (π_+^*,π_-^*) per bond. Based on this finding, it is predicted that the staffane bridges should be more effective than the polynorbornyl bridges at propagating electronic interactions over long distances, *including intramolecular electron transfer and energy transfer processes*. It is demonstrated, by means of a natural bond orbital analysis, that interactions that skip over bonds are very important for describing the coupling between adjacent staffane units.

I. Introduction

Oligo[1.1.1]propellanes, or [n]staffanes, **[n]1**, are receiving considerable attention on account of their potential application as molecular building blocks for the construction of novel materials.[1-5] One such application offered by end-functionalized staffanes, having the general structure shown by **[n]1**, lies in the

[n]1

ability of the oligomeric hydrocarbon bridge or spacer to hold the two end groups, X and Y, at well-defined separations. Such systems should be ideal for studying the dynamics and efficiency of long-range intramolecular electron transfer (ET) and energy transfer processes between the chromophores X and Y.

Long-range intramolecular ET, in particular, continues to generate considerable activity,[6] and a variety of rigid, donor–{saturated hydrocarbon bridge}–acceptor systems has been synthesized and used in ET studies. Hydrocarbon bridges that have been employed in such studies include cyclohexane, decalin, and steroid-based systems,[7,8] bicyclo[2.2.2]octane,[9] triptycene,[10] polyspirocyclobutanes,[11] and norbornylogous bridges, such as **2(m,n)**,

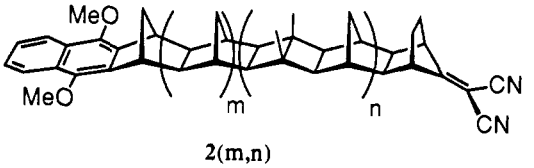

2(m,n)

comprising linearly fused norbornyl and bicyclo[2.2.0]hexyl groups.[12] Such studies have verified the crucial role played by the bridge in mediating long-range intramolecular ET. For

† University of New South Wales.
§ University of Pittsburgh.

(1) (a) Wiberg, K. *Chem. Rev.* **1989**, *89*, 975. (b) Semmler, K.; Szeimies, G.; Belzner, J. *J. Am. Chem. Soc.* **1985**, *107*, 6410.
(2) Kaszynski, P.; Friedli, A. C.; Michl, J. *J. Am. Chem. Soc.* **1992**, *114*, 601, and references cited therein.
(3) Bunz, U.; Polborn, K.; Wagner, H.-U.; Szeimes, G. *Chem. Ber.* **1988**, *121*, 1785.
(4) Gleiter, R.; Szeimies, G.; Bunz, U. *Angew. Chem., Int. Ed. Engl.* **1990**, *29*, 413.
(5) Schafer, O.; Allan, M.; Szeimies, G.; Sanktjohanser, M. *Chem. Phys. Lett.* **1992**, *195*, 293.
(6) (a) Wasielewski, M. R. *Photoinduced Electron Transfer*, Part D; Fox, M. A., Chanon, M. Eds.; Elsevier: Amsterdam, 1988; Chapter 1.4. (b) Miller, J. R.; Closs, G. L. *Science* **1988**, *240*, 440. (c) Paddon-Row, M. N.; Verhoeven, J. W. *New J. Chem.* **1991**, *15*, 107.
(7) (a) Calcaterra, L. T.; Closs, G. L.; Miller, J. R. *J. Am. Chem. Soc.* **1983**, *105*, 670. (b) Miller, J. R.; Calcaterra, L. T.; Closs, G. L. *J. Am. Chem. Soc.* **1984**, *106*, 3047. Closs, G. L.; Calcaterra, L. T.; Green, N. J.; Penfield, K. W.; Miller, J. R. *J. Phys. Chem.* **1986**, *90*, 3673.
(8) (a) Pasman, P.; Verhoeven, J. W.; de Boer, Th. *Chem. Phys. Lett.* **1978**, *59*, 381. (b) Pasman, P.; Rob, F.; Verhoeven, J. W. *J. Am. Chem. Soc.* **1982**, *104*, 5127. (c) Pasman, P.; Mes, G. F.; Koper, N. W.; Verhoeven, J. W. *J. Am. Chem. Soc.* **1985**, *107*, 5839.
(9) (a) Joran, A. D.; Leland, B. A.; Geller, G. G.; Hopfield, J. J.; Dervan, P. B. *J. Am. Chem. Soc.* **1984**, *106*, 6090. (b) Joran, A. D.; Leland, B. A.; Felker, P. M.; Zewail, A. H.; Leland, B. A.; Joran, A. D.; Felker, P. M.; Zewail, A. H.; Hopfield, J. J.; Dervan, P. B. *J. Phys. Chem.* **1985**, *89*, 557.
(10) (a) Wasielewski, M. R.; Niemczyk, M. P.; Svec, W. A.; Pewitt, E. B. *J. Am. Chem. Soc.* **1985**, *107*, 5562. (b) Wasielewski, M. R.; Niemczyk, M. P.; Johnson, D. G.; Svec, W. A.; Minsek, D. W. *Tetrahedron* **1989**, *45*, 4785. (c) Wasielewski, M. R.; Niemczyk, M. P.; Svec, W. A.; Pewitt, E. B. *J. Am. Chem. Soc.* **1985**, *107*, 1080.
(11) (a) Stein, C. A.; Taube, H. *J. Am. Chem. Soc.* **1981**, *103*, 693. (b) Stein, C. A.; Lewis, N. A.; Seitz, G. *J. Am. Chem. Soc.* **1982**, *104*, 2596.

0002-7863/93/1515-2952$04.00/0

Scheme I

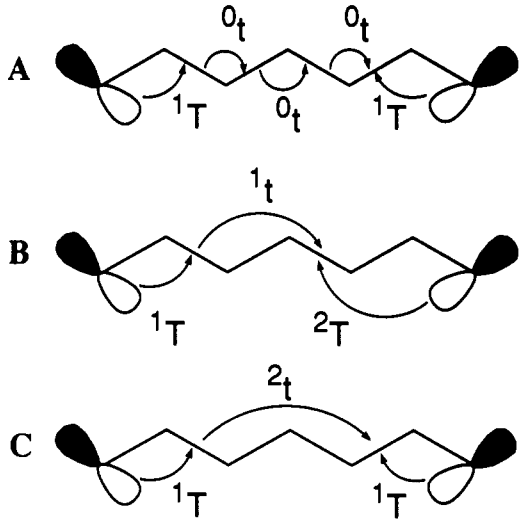

example, it was found that the norbornylogous bridge system in **2(m,n)** mediated unprecedented rapid rates of intramolecular ET (in excess of 10^9 s^{-1}) over distances as great as 14 Å.[12] The bridge-mediated ET process is thought to be due to a through-bond (TB) coupling mechanism,[13] in which the orbitals of the donor and acceptor chromophores interact with each other via their mutual coupling with the σ and σ^* orbitals of the intervening saturated bridge. TB coupling is relevant within the context of ET when the latter occurs under nonadiabatic conditions (which is generally the case for long-range ET occurring over distances >7 Å). Under these conditions, application of the Golden Rule leads to the following expression for the rate constant for ET, k_{et}:

$$k_{et} = (4\pi^2/h)|H_{DA}|^2\text{FCWD} \qquad (1)$$

where H_{DA} is the electronic interaction matrix element between donor, D, and acceptor, A, and FCWD denotes the Franck–Condon weighted density of states.[14]

The dynamics of long-range ET and the distance dependence of ET rates depend sensitively on the magnitude of the H_{DA} matrix element which, in turn, is largely determined by the strength of the TB coupling involving the donor and acceptor group orbitals. The overall strength of TB coupling depends on both the degree of coupling between the orbitals of each chromophore with those of the bridge (as indicated by the arrows labeled ^1T and ^2T in Scheme I), and on the strength of the coupling of the bridge orbitals with each other (as indicated by the arrows labeled ^0t, ^1t, and ^2t in the scheme). The latter "intrabridge" orbital coupling is particularly important in that it largely determines the distance dependence characteristics of intramolecular ET processes.

A fruitful way of exploring the efficacy of a bridge for mediating ET via the TB mechanism in donor–bridge–acceptor systems is to examine models in which the donor and acceptor groups are replaced by simpler chromophores, such as double and triple bonds. Thus, the C_{2v} dienes, **3(2)**–**3(6)** (the numbers in parentheses refer

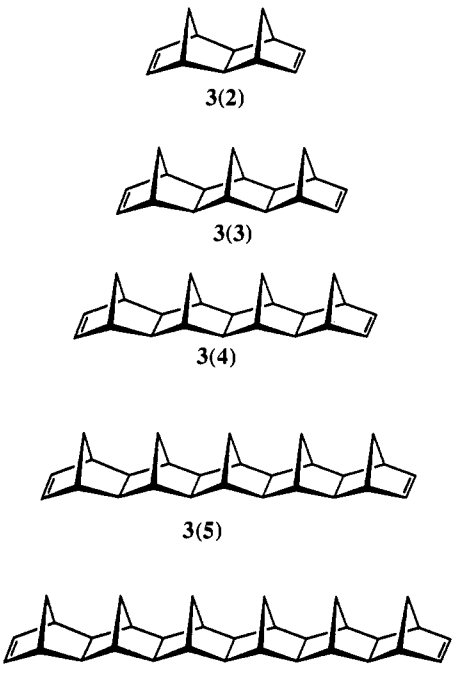

to the number of fused norbornyl units), have been used to model TB coupling in the more complicated bichromophoric molecules, **2(m,n)**, in which the bridge length varies from 4 to 12 bonds, in two-bond increments.[15-18] Orbital interactions in such dienes are manifested through splittings of the π and π^* levels, the magnitude of which is taken as a direct measure of the strength of the orbital couplings. These splits may be conveniently determined either experimentally, through measurement of the π ionization potentials (by photoelectron spectroscopy[19,20]) and the π^* electron affinities (by electron transmission spectroscopy,[21,22]), or computationally, particularly through Koopmans' theorem[23] calculations using ab initio MO theory.

It has been found,[16] for example, that the distance dependence of the π_+^*,π_-^* splitting energies obtained from the STO-3G minimum basis set calculations on the dienes **3(2)**–**3(5)** is remarkably similar to the distance dependence of H_{DA} (see eq 1), deduced from the observed rates of photoinduced ET in the more complex systems, **2(m,n)**.[12] This correspondence suggests that this model-compound approach may have more general applicability for investigating the ability of various bridges to act as mediators of ET processes.

(12) (a) Penfield, K. W.; Miller, J. R.; Paddon-Row, M. N.; Cotsaris, E.; Oliver, A. M.; Hush, N. S. *J. Am. Chem. Soc.* **1987**, *109*, 5061. (b) Hush, N. S.; Paddon-Row, M. N.; Cotsaris, E.; Oevering, H.; Verhoeven, J. W.; Heppener, M. *Chem. Phys. Lett.* **1985**, *117*, 8. (c) Warman, J. M.; de Haas, M. P.; Paddon-Row, M. N.; Cotsaris, E.; Hush, N. S.; Oevering, H.; Verhoeven, J. W. *Nature (London)* **1986**, *320*, 615. (d) Warman, J. M.; de Haas, M. P.; Oevering, H.; Verhoeven, J. W.; Paddon-Row, M. N.; Oliver, A. M.; Hush, N. S. *Chem. Phys. Lett.* **1986**, *128*, 95. (e) Oevering, H.; Paddon-Row, M. N.; Heppener, M.; Oliver, A. M.; Cotsaris, E.; Verhoeven, J. W.; Hush, N. S. *J. Am. Chem. Soc.* **1987**, *109*, 3258. (f) Paddon-Row, M. N., Oliver, A. M.; Warman, J. M.; Smit, K. J.; de Haas, M. P.; Oevering, H.; Verhoeven, J. W. *J. Phys. Chem.* **1988**, *92*, 6958. (g) Oliver, A. M.; Craig, D. C.; Paddon-Row, M. N.; Kroon, J.; Verhoeven, J. W. *Chem. Phys. Lett.*, **1988**, *150*, 366. (h) Lawson, J. M.; Craig, D. C.; Paddon-Row, M. N.; Kroon, J.; Verhoeven, J. W. *Chem. Phys. Lett.* **1989**, *164*, 120. (i) Oevering, H.; Verhoeven, J. W.; Paddon-Row, M. N.; Warman, J. M. *Tetrahedron* **1989**, *45*, 4751. (j) Kroon, J.; Verhoeven, J. W.; Paddon-Row, M. N.; Oliver, A. M. *Angew Chem., Int. Ed. Engl.* **1991**, *30*, 1358. (k) Antolovich, M.; Keyte, P. J.; Oliver, A. M.; Paddon-Row, M. N.; Kroon, J.; Verhoeven, J. W.; Jonker, S. A.; Warman, J. M. *J. Phys. Chem.* **1991**, *95*, 1933.

(13) (a) Hoffmann, R.; Imamura, A.; Hehre, W. J. *J. Am. Chem. Soc.* **1968**, *90*, 1499. (b) Hoffmann, R. *Acc. Chem. Res.* **1971**, *4*, 1. (c) Gleiter, R. *Angew. Chem., Int. Ed. Engl.* **1974**, *13*, 696. (d) Paddon-Row, M. N. *Acc. Chem. Res.* **1982**, *15*, 245.

(14) Marcus, R. A.; Sutin, N. *Biochim. Biophys. Acta* **1985**, *811*, 265.

(15) Paddon-Row, M. N.; Jordan, K. D. In *Modern Models of Bonding and Delocalization*; Liebman, J. F., Greenberg, A., Eds.; VCH Publishers: New York, 1988; p 10.

(16) Paddon-Row, M. N.; Wong, S. S. *Chem. Phys. Lett.* **1990**, *167*, 432.

(17) Jordan, K. D.; Paddon-Row, M. N. *J. Phys. Chem.* **1992**, *96*, 1188.

(18) Jordan, K. D.; Paddon-Row, M. N. *Chem. Rev.* **1992**, *92*, 395.

(19) (a) Paddon-Row, M. N.; Patney, H. K.; Brown, R. S.; Houk, K. N. *J. Am. Chem. Soc.* **1981**, *103*, 5575. (b) Jørgensen, F. A.; Paddon-Row, M. N.; Patney, H. K. *J. Chem. Soc., Chem. Commun.* 1983, 573. (c) Paddon-Row, M. N.; Patney, H. K.; Peel, J. B.; Willett, G. D. *J. Chem. Soc., Chem. Commun.* 1984, 564.

(20) Martin, H.-D.; Mayer, B. *Angew. Chem., Int. Ed. Engl.* **1983**, *22*, 283. Gleiter, R.; Schaefer, W. *Acc. Chem. Res.* **1990**, *23*, 369.

(21) Jordan, K. D.; Burrow, P. D. *Chem. Rev.* **1987**, *87*, 557.

(22) Balaji, V.; Ng, L.; Jordan, K. D.; Paddon-Row, M. N.; Patney, H. K. *J. Am. Chem. Soc.* **1987**, *109*, 6957.

(23) Koopmans, T. *Physica* **1934**, *1*, 104.

It is in this spirit that we decided to investigate TB coupling in the diethynyl[n]staffanes, **4(1)**–**4(5)**,[24] using ab initio MO

4(1)

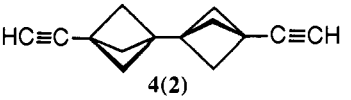

4(2)

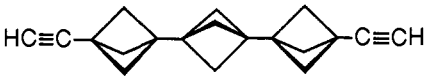

4(3)

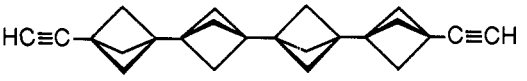

4(4)

4(5)

theory. Our interest in these molecules was prompted by the appearance of two experimental investigations on π,π and π^*,π^* orbital interactions in the first member of the series, **4(1)**.[4,5] The diethynyl[n]staffanes have two pairs of degenerate π orbitals, designated π_+ and π_-, and two pairs of degenerate π^* orbitals, designated $\pi_+{}^*$ and $\pi_-{}^*$, where the "+" and "–" refer to the in-phase and out-of-phase combinations of π (or π^*) orbitals localized on the left- and right-hand acetylenic groups, respectively. The photoelectron spectrum[4] of **4(1)** shows two peaks split by 0.68 eV, due to ionization from the π_+ and π_- orbitals, and the electron transmission spectrum[5] shows two peaks, split by 1.12 eV, due to electron capture into the $\pi_+{}^*$ and $\pi_-{}^*$ orbitals. These large splittings, which have been confirmed by prior theoretical calculations,[4,5,25] must be due almost entirely to TB interactions, since the separation between the two acetylenic groups is sufficiently large that the through-space (TS) interactions must be negligible (<0.1 eV). The calculations presented herein will allow us to determine the effectiveness of staffane bridges for propagating electronic interactions over distances as great as 19 Å.

Because different authors define TB and TS differently, it is important to make clear the context within which these terms are employed in the present work. We reserve the term "through-space" for the direct interaction between the orbitals of the acetylenic groups, and refer to all other coupling mechanisms between the two chromophores as "through-bond". With this definition, in addition to the "normal" TB pathway, illustrated by **A** in Scheme I, involving interactions between adjacent bonds, pathways in which there are interactions "skipping" over bonds of the bridges (e.g., **B** and **C** in Scheme I), are also classified as TB in nature. To the extent that the TB coupling proceeds via a series of interactions between adjacent bonds, a minimal basis set should be adequate for calculating the splittings. However, to the extent to which pathways involving interactions that skip over bonds are important, it will be necessary to employ more flexible basis sets. The need for flexible basis sets will be especially acute when there are important interactions that skip over two or more bonds.

In this work, we focus on the splittings between the two π cation states, Δ_{IP}, and those between the two π^* anion states, Δ_{EA}, as measures of the electronic coupling. The Δ_{IP} and Δ_{EA} values are calculated in the Koopmans' theorem (KT) approximation, in which they are associated, respectively, with the π_+,π_- and $\pi_+,{}^*\pi_-{}^*$ splittings obtained from Hartree–Fock (HF) calculations on the neutral molecules. We, and others, have shown that the KT splittings can faithfully reproduce the trends in the Δ_{IP} and Δ_{EA} values along a series of chromophore–bridge–chromophore compounds.[15-18,25] In order to gain insight into the nature of the interactions responsible for the TB couping in the π and π^* manifolds of **4(1)**–**4(5)**, the HF calculations are performed with basis sets of different radial extents, and an analysis of orbital interactions is carried out in terms of localized natural bond orbitals (NBO's).[26]

II. Computational Methodology

The geometries of **4(1)**–**4(5)** were optimized[27] at the HF level of theory, using both the STO-3G and the 3-21G basis sets.[28] Symmetry constraints used for the optimizations were D_{3h} for the odd-numbered staffanes, **4(1)**, **4(3)**, and **4(5)**, and D_{3d} for the even-numbered members.[29] Single-point energy calculations were then carried out on the optimized geometries using the STO-3G, 3-21G, and 6-31G* basis sets.[28] The STO-3G basis set, due to its "minimal" nature, is inadequate for describing interactions occurring over distances much greater than 3 Å, e.g., that depicted by ^{2}t in part C of Scheme I. The 3-21G and 6-31G* split-valence basis sets are suitable for describing longer range interactions (up to about 4.5 Å), with the 6-31G* basis set expected to be slightly better in this regard (because its outermost carbon sp function is somewhat more diffuse). Comparison of the π_+,π_- and $\pi_+,{}^*\pi_-{}^*$ splittings obtained with these three basis sets thus provides an indication of the importance of interactions between nonadjacent bonds.

HF calculations were also carried out on **4(1)**–**4(3)** using the 6-31G, 6-311G, and D95v basis sets.[28] Comparison of the results obtained with the 6-31G and 6-31G* basis sets allows us to determine whether the d polarization functions in the latter basis set are important for describing the π_+,π_- or $\pi_+,{}^*\pi_-{}^*$ splittings. The results obtained with the 6-311G and D95v basis sets permit us to determine whether interactions of even longer range than can be accounted for by the 6-31G basis set make significant contributions to the TB coupling.

In order to gain further insight into the nature of the interactions responsible for the TB coupling in these compounds, the canonical HF orbitals were localized to give natural bond orbitals (NBO's),[26] and the NBO's were used to determine the relative importance of various coupling pathways. A more detailed discussion of the NBO pathway approach, as applied to the analysis of TB interactions, may be found in refs 18, 25, 30, and 31.

III. Results

Table I summarizes for **4(1)**–**4(5)** the π_+,π_- splittings obtained with the STO-3G, 3-21G, and 6-31G* basis sets for both the

(24) The numbers in parentheses refer to the number of bicyclo[1.1.1]-pentyl units in the relay. In contrast to the usual notation for staffanes (e.g., [n]**1**), the parenthetical descriptor has been placed after the structure number, in **4**(n), for the sake of being consistent with the notation used for the polynorbornyl systems, **3**(n).

(25) Liang, C.; Newton, M. *J. Phys. Chem.* **1992**, *96*, 2855.

(26) (a) Reed, A. E.; Curtiss, L. A.; Weinhold, F. *Chem. Rev.* **1988**, *88*, 899. (b) Reed, A. E.; Weinhold, F. *J. Chem. Phys.* **1985**; *83*, 1736.

(27) The GAUSSIAN 90 suite of programs was used for all computational work: GAUSSIAN 90, Revision H: Frisch, M. J.; Head-Gordon, M.; Trucks, G. W.; Foresman, J. B.; Schlegel, H. B.; Raghavachari, K.; Robb, M.; Binkley, J. S.; Gonzalez, C.; Defrees, D. J.; Fox, D. J.; Whiteside, R. A.; Seeger, R.; Melius, C. F.; Baker, J.; Martin, R. L.; Kahn, L. R.; Stewart, J. J. P.; Topiol, S.; Pople, J. A. Gaussian, Inc.: Pittsburgh PA, 1990.

(28) For a discussion of the STO-3G, 3-21G, 6-31G, 6-31G*, and 6-311G basis sets, as well as citations to the original literature, see: Hehre, W. J.; Radom, L.; Schleyer, P. v. R.; Pople, J. A. *Ab Initio Molecular Orbital Theory*; John Wiley: New York, 1986. (b) The D95v basis set is described in: Dunning, T. H. *J. Chem. Phys.* **1970**, *53*, 2823.

(29) Harmonic vibrational frequency calculations carried out analytically at the HF/STO-3G level of theory on the STO-3G optimized structures of **4(1)** and **4(2)** gave all real frequencies, showing that they correspond to minimum energy species.

(30) Naleway, C. A.; Curtiss, L. A.; Miller, J. R. *J. Phys. Chem.* **1991**, *95*, 8434.

(31) (a) Paddon-Row, M. N.; Jordan, K. D. *J. Chem. Soc., Chem. Commun.* 1988, 1508. (b) Paddon-Row, M. N.; Wong, S. S.; Jordan, K. D. *J. Am. Chem. Soc.* **1990**, *112*, 1710. (c) Paddon-Row, M. N.; Wong, S. S.; Jordan, K. D. *J. Chem. Soc., Perkin Trans. 2* **1990**, 417.

Table I. π_+,π_- Splitting Energies (eV) and $\beta_h(i,i+1)$ Values (per Bond) Determined from the Splittings for **4(i)** and **4(i+1)**[a]

molecule	STO-3G	3-21G	6-31G*	6-31G	D95v	6-311G
4(1)	0.57 (0.52)	0.68 (0.63)	0.69 (0.64)	(0.63)	(0.64)	(0.64)
4(2)	0.17 (0.15)	0.28 (0.25)	0.27(0.24)	(0.24)	(0.25)	(0.26)
4(3)	0.059 (0.049)	0.13 (0.11)	0.12 (0.10)	(0.105)	(0.12)	(0.115)
4(4)	0.021 (0.017)	0.068 (0.054)	0.058 (0.046)			
4(5)	0.0079 (0.006)	0.038 (0.028)	0.030 (0.022)			
$\beta_h(1,2)$	0.40 (0.41)	0.30 (0.31)	0.31 (0.33)	(0.32)	(0.31)	(0.30)
$\beta_h(2,3)$	0.36 (0.38)	0.25 (0.27)	0.27 (0.29)	(0.28)	(0.24)	(0.27)
$\beta_h(3,4)$	0.34 (0.36)	0.22 (0.24)	0.24 (0.26)			
$\beta_h(4,5)$	0.33 (0.35)	0.20 (0.22)	0.22 (0.25)			

[a] The 3-21G results are given first, followed by the STO-3G results in parentheses.

Table II. π_+^*,π_-^* Splitting Energies (eV) and $\beta_e(i,i+1)$ Values (per Bond) Determined from the Splittings for **4(i)** and **4(i+1)**[a]

molecule	STO-3G	3-21G	6-31G*	6-31G	D95v
4(1)	0.23 (0.21)	0.97 (0.97)	1.02 (1.03)	(0.98)	(0.885)
4(2)	0.017 (0.014)	0.31 (0.31)	0.37 (0.38)	(0.37)	(0.30)
4(3)	0.0011 (0.00082)	0.11 (0.10)	0.15 (0.16)	(0.15)	(0.10)
4(4)	$<10^{-4}$ ($<10^{-4}$)	0.035 (0.034)	0.058 (0.061)		
4(5)	$<10^{-4}$ ($<10^{-4}$)	0.011 (0.011)	0.022 (0.024)		
$\beta_e(1,2)$	0.88 (0.92)	0.38 (0.38)	0.34 (0.33)	(0.32)	(0.36)
$\beta_e(2,3)$	0.91 (0.94)	0.36 (0.37)	0.31 (0.30)	(0.30)	(0.36)
$\beta_e(3,4)$		0.37 (0.37)	0.32 (0.31)		
$\beta_e(4,5)$		0.37 (0.37)	0.32 (0.31)		

[a] The 3-21G results are given first, followed by the STO-3G results in parentheses.

3-21G and STO-3G optimized geometries, and Table II summarizes the corresponding results for the π_+^*,π_-^* splittings. Both the π_+,π_- and π_+^*,π_-^* splittings are somewhat larger at the 3-21G than at the STO-3G optimized geometries, but these differences are relatively small, and for the remainder of this study, unless noted otherwise, we will focus on results obtained atthe HF/3-21G optimized geometries. We note also that the π_+,π_- and π_+^*,π_-^* splittings obtained for **4(1)**–**4(3)** using the 6-31G basis set are nearly identical with those obtained using the 6-31G* basis set, showing that the d polarization functions in the latter are unimportant for describing the TB interactions. Thus, we can assume that differences between the splittings calculated with the 3-21G and 6-31G* basis sets are due primarily to the more radially extended s and p functions in the latter basis set.

A. π_+,π_- Splittings. The π_+,π_- splittings calculated with the 3-21G basis set are larger than those calculated with the STO-3G basis set, with the ratio of the 3-21G to STO-3G splittings increasing monotonically with bridge length, from a value of 1.19 for **4(1)** to 4.81 for **4(5)**. This suggests that interactions of longer range than can be adequately treated by the STO-3G basis set are important for describing the propagation of the interactions along the bridge. With the exception of **4(1)**, the π_+,π_- splittings calculated with the 6-31G* basis set are somewhat smaller than those obtained with the 3-21G basis set, with the percentage reduction increasing with bridge length. Calculations on **4(1)**–**4(3)** with the 6-311G and D95v basis sets gave π_+,π_- splittings nearly identical with those obtained with the 6-31G* basis set, indicating that interactions of longer range than can be described with the 6-31G* basis set are unimportant for describing the TB coupling between the localized π orbitals in these compounds.

B. π_+^*,π_-^* Splittings. From examination of Table II, it is seen that the π_+^*,π_-^* splittings calculated with the 3-21G basis set range from a factor of 4.2 (for **4(1)**), to roughly a factor of 10^2 (for **4(5)**) larger than those obtained with the STO-3G basis set. Clearly, the STO-3G basis set does not provide even a qualitatively correct description of the TB coupling in the π^* manifold. The changes in the π_+^*,π_-^* splittings introduced in going from the 3-21G to the 6-31G* basis set are much less dramatic, with the ratios of the 6-31G* to 3-21G π_+^*,π_-^* splittings increasing from 1.05 for **4(1)** to 2.00 for **4(5)**.

Given the changes in the π_+^*,π_-^* splittings in going from the 3-21G to the 6-31G* basis sets, it is natural to wonder whether these splittings would be increased even further upon the adoption of still more flexible basis sets. However, this is difficult to determine because HF calculations with flexible basis sets give rise to low-lying virtual orbitals which correspond to approximations to continuum functions as well as to negative anion states in a Koopmans' theorem sense.[32] For sufficiently flexible basis sets, the lowest-lying unfilled orbitals will, in fact, correspond to approximations to continuum functions. This problem occurs, for example, for the 6-311G basis set, and it is for this reason that π_+^*,π_-^* splittings are not reported for this basis set. With the D95v basis set, on the other hand, the lowest unfilled orbitals do correspond to anion states in a KT sense, although the energy separations between these virtual orbitals and those corresponding to approximations to continuum functions (of the same symmetry) are only a few electron volts.[33]

Surprisingly, the π_+^*,π_-^* splittings obtained with the D95v basis set are closer to those obtained with the 3-21G than with the 6-31G* basis set. However, this could be due to an unphysical mixing between the two types of unfilled orbitals in the D95v basis set. In support of the use of the 6-31G* basis set for studying the TB coupling between the π^* orbitals, we note that the π_+^*,π_-^* splitting of **4(1)**, calculated with the 6-31G* basis set, 1.02 eV, is in excellent agreement with the splitting (1.1 eV) measured experimentally between the two π^* anion states.[5]

C. Distance Dependence of the π_+,π_- and π_+^*,π_-^* Splittings. The simplest model for describing the TB coupling between two equivalent chromophores is the McConnell model,[34] illustrated by **A** in Scheme I, in which the π_+,π_- (π_+^*,π_-^*) splitting, ΔE, is defined as:

$$\Delta E = -2\left\{\frac{T^2}{\Delta}\right\}\left\{\frac{t}{\Delta}\right\}^{m-1} \qquad (2)$$

where T gives the coupling of the chromophore to the bridge, t gives the coupling between adjacent bridge sites, Δ is the energy gap between the relevant localized orbital of the chromophore

(32) Falcetta, M. F.; Jordan, K. D. *J. Am. Chem. Soc.* **1991**, *113*, 2903.

(33) Note that while the outermost carbon p function in the D95v basis set is considerably more diffuse than that in the 6-31G basis set, the outermost carbon sp function in the 6-311G basis set is only slightly more diffuse than that in the 6-31G basis set. Thus, it is the presence of the extra set of sp functions in the 6-311G basis set, rather than the "diffuseness" of the basis functions, which leads to the low-energy "continuum" solutions in this case.

(34) McConnell, H. M. *Chem. Phys.* **1961**, *35*, 508.

and that of one of the bridge sites, and m is the number of bridge sites. This model assumes that there is a single orbital of importance on each chromophore and on each bridge site, that all bridge sites are identical, and that only nearest-neighbor interactions are important. Clearly, these assumptions are not valid for the compounds **4(1)**–**4(5)**. Still, to the extent that a staffane subunit can be thought of as a single "effective" filled or unfilled orbital, one might expect the McConnell theory to hold approximately.

A particularly physically appealing attribute of the McConnell model is that the net splitting is expressed as a product of a term describing the coupling of the chromophore to the bridge and a term describing the propagation of the interaction along the bridge. In this model, the ratio of the splittings for consecutive members of a series of chromophore–(bridge)$_m$–chromophore compounds is a constant and equal to $(t/\Delta)^{\Delta m}$, where Δm is the number of active bonds in a single bridge unit. Equivalently, eq 2 is consistent with an exponential dependence of the splitting on the bridge length, commonly expressed as:

$$\Delta E = A \exp(-\beta m) \qquad (3)$$

A test of the validity of the McConnell model for a series of chromophore–(bridge)$_m$–chromophore compounds is provided by determining whether the β values obtained by using the splittings from successive pairs of molecules in the series are equal. In this work, the β values obtained from the π_+,π_- and π_+^*,π_-^* splittings are referred to as β_h and β_e, respectively (where the "h" and "e" subscripts denote hole and electron transfer processes, respectively).

In using eqs 2 or 3, it is necessary to establish a scheme for counting the bridge sites, i.e., for determining m. However, because we are interested in the β values (and not in the A parameters), we actually need only to specify the increment, Δm, between successive members of the series, and it is irrelevant whether the C–C σ bonds between the terminal staffane rings and the acetylenic groups are countered. In this work, we choose m to be equal to the total number of C–C bonds in one of the relays connecting the two acetylenic groups. Thus, $m = 7$ for **4(2)**. In this counting scheme, the increment, Δm, between consecutive members of the series is 3. This means that we are also including those bonds connecting the staffane units even though, by symmetry, the localized C–C σ and σ^* orbitals associated with these bonds cannot mix with the π or π^* orbitals. If these bonds were not counted, so that $\Delta m = 2$, or if each staffane unit were counted as a single site, so that $\Delta m = 1$, then different β values would obviously result; of course, conclusions about the constancy (or lack thereof) of the β values along the series of molecules **4(1)**–**4(5)** would not be altered. However, the selected counting scheme has the important advantage that it facilitates comparison of β values for different bridges since they each refer to the total length of the respective bridge (in terms of the total number of component σ bonds).

The β_h and β_e values (per bond) calculated using the π_+,π_- and π_+^*,π_-^* splittings for successive members of the series **4(1)**–**4(5)** are summarized in Tables I and II, respectively. For each of the STO-3G, 3-21G, and 6-31G* basis sets, the β_h values are found to decrease monotonically with increasing bridge length, with the difference between successive β_h values becoming smaller as one progresses along the series of molecules. The β_h values obtained with the 3-21G and 6-31G* basis sets are nearly the same and are significantly smaller than those obtained with the STO-3G basis set. The spreads in the β_h values are somewhat greater with the 3-21G and 6-31G* basis sets than with the STO-3G basis set. With the split-valence basis sets, the β_h values obtained from the π_+,π_- splittings of **4(4)** and **4(5)** are about two-thirds as large as those obtained from the π_+,π_- splittings of **4(1)** and **4(2)**.

The β_e values are consistently larger than the corresponding β_h values, indicating that the TB coupling falls off more rapidly with increasing bridge length in the π^* than in the π manifold. Unlike the situation found for the β_h values, the β_e values are nearly constant along the sequence of molecules **4(1)**–**4(5)**. Because the STO-3G π_+^*,π_-^* splittings drop off so rapidly with increasing bridge length, only the first two β_e values, $\beta_e(1,2)$ and $\beta_e(2,3)$, can be determined with this basis set. The resulting β_e values are about 2.5 times larger than the corresponding 3-21G values.

Table III. π_+,π_- Splitting Energies (eV) and $\beta_h(i,i+1)$ Values (per Bond) Determined from the Splittings for **3(i)** and **3(i+1)**[a]

molecule	STO-3G	3-21G
3(2)	0.99	1.06
3(3)	0.35	0.38
3(4)	0.14	0.17
3(5)	0.065	0.085
3(6)	0.029	0.043
$\beta_h(2,3)$	0.51	0.48
$\beta_h(3,4)$	0.45	0.42
$\beta_h(4,5)$	0.39	0.33
$\beta_h(5,6)$	0.39	0.34

[a] Values are for the 3-21G optimized geometries.

Table IV. π_+^*,π_-^* Splitting Energies (eV) and $\beta_e(i,i+1)$ Values (per Bond) Determined from the Splittings for **3(i)** and **3(i+1)**[a]

molecule	STO-3G	3-21G
3(2)	0.85	0.90
3(3)	0.23	0.18
3(4)	0.066	0.091
3(5)	0.019	0.032
3(6)	0.0057	0.011
$\beta_e(2,3)$	0.69	0.75
$\beta_e(3,4)$	0.60	0.35
$\beta_e(4,5)$	0.59	0.52
$\beta_e(5,6)$	0.60	0.55

[a] Values are for the 3-21G optimized geometries.

D. Comparison of the Trends in the π_+,π_- and π_+^*,π_-^* Splittings in 4(1)-4(5) to Those in the Polynorbornyl Dienes, 3(2)–3(6). It is instructive to compare the trends in the β values for **4(1)**–**4(5)** to those for the series of polynorbornyl dienes, **3(2)**–**3(6)**. The STO-3G and 3-21G values of the π_+,π_- and π_+^*,π_+^*,π_-^* splittings, together with the associated β values for the polynorbornyl systems, are summarized in Tables III and IV. In both series of molecules, the β_h values decrease with increasing chain length, with the rate of decrease being somewhat greater with split-valence basis sets than with the minimal basis set. In addition, for both series of molecules the β_h values appear to converge as one progresses to longer members of the series. The β_h values calculated with the 3-21G basis set are consistently smaller than those calculated with the STO-3G basis set, with the decreases in the β_h values due to the adoption of the more flexible basis set being more pronounced for **4(1)**–**4(5)** than for **3(2)**–**3(6)**.

With the 3-21G and other split-valence basis sets, the π_+^*,π_-^* splitting for **3(3)** is anomalously small, causing the β_e value calculated from the π_+^*,π_-^* splittings of **3(2)** and **3(3)** to be especially large and that calculated from the π_+^*,π_-^* splittings of **3(3)** and **3(4)** to be especially small.[17] Ignoring this exception, the β_e values for both classes of molecules tend to be relatively independent of the bridge length and to be smaller when calculated with the 3-21G than with the STO-3G basis set. The basis set dependence is much more pronounced for the β_e values associated with the staffane bridges than those associated with the polynorbornyl bridges.

IV. NBO Analyses

The Hartree–Fock MO calculations on **4(1)**–**4(5)** provide relatively little insight into the factors responsible for the magnitudes of the π_+,π_- and π_+^*,π_-^* splittings and their

dependencies on the bridge length. As a means of gaining deeper insight, we use an approach in which the canonical HF orbitals are localized and the π_+,π_- and π_+^*,π_-^* splittings are then obtained from calculations retaining only subsets of the localized orbitals. This approach, which allows one to determine the importance of various localized orbitals for the TB coupling, was pioneered by the Heilbronner and Imamura groups,[35] and used by us[18,31] in analyzing the π_+,π_- and π_+^*,π_-^* splittings of several substituted norbornadienes and the polynorbornyl dienes **3(2)–3(6)**. The relative importance of various "pathways" depends somewhat on the choice of the localization procedure. However, because our goal is to develop a qualitative understanding of the nature of the interactions responsible for the trends in the splittings, we are not concerned with the sensitivity to the choice of the localized orbitals. In the present study we have adopted as localized orbitals the natural bond orbitals (NBO's) of Weinhold and co-workers,[26] used by us,[31] and subsequently by other groups[25,30,36] to study the consequences of TB coupling through saturated bridges.

In order to obtain the energies of the π_+ and π_- (π_+^* and π_-^*) orbitals in the absence of TB coupling, we first diagonalize the 2×2 Hamiltonian matrix involving the localized π (or π^*) NBO's. The resulting orbitals are designated $^{SL}\pi_+$, $^{SL}\pi_-$, $^{SL}\pi_+^*$, and $^{SL}\pi_-^*$, where the "SL" superscript implies that these are symmetry-adapted semilocalized orbitals. For all the molecules **4(1)–4(5)**, the $^{SL}\pi_+$ and $^{SL}\pi_-$ orbitals obtained via this approach are nearly degenerate. The same is true for the $^{SL}\pi_+^*$ and $^{SL}\pi_-^*$ orbitals. These results indicate that, as expected, TS interactions between the acetylenic groups are relatively unimportant.

We then considered interactions of the $^{SL}\pi$ and $^{SL}\pi^*$ orbitals with subsets of the σ and σ^* NBO's. These calculations were carried out using two different approaches. In both approaches the π_+,π_- and π_+^*,π_-^* splittings were estimated by diagonalizing NBO matrices containing selected subsets of the interactions. In the first approach, only results obtained with the 3-21G basis set are considered, and the NBO matrices were built up by successively adding, in groups, all C–C σ, C–H σ, C–C σ^*, C–H σ^*, and the so-called "Rydberg" orbitals.[37] In applying this approach to the π^* manifold, the initial subspace actually includes the appropriate "Rydberg" NBO's as well as the π^* NBO's.[38] When a group of orbitals is added, all interactions involving these orbitals with one another and with all NBO's already present are included. In this approach no effort is made to separate interactions into short versus long range. In the second approach, to be described below, subsets of the C–C σ and C–C σ^* interactions are selected according to the "range" of the interactions.

In applying the first of these approaches to the analysis of the influence of TB coupling on the energies of the π orbitals, we first mix the $^{SL}\pi$ orbitals with the C–C σ NBO's, followed, in succession, by addition of the interactions involving the C–H σ NBO's, core NBO's, C–C σ^* NBO's, C–H σ^* NBO's, and the "Rydberg" NBO's. Similarly, in the analysis of the TB mixing in the π^* manifold, the sequence in which the NBO's are mixed is: C–C σ^*, C–H σ^*, "Rydberg", C–C σ, and, together, the C–H σ and core NBO's.

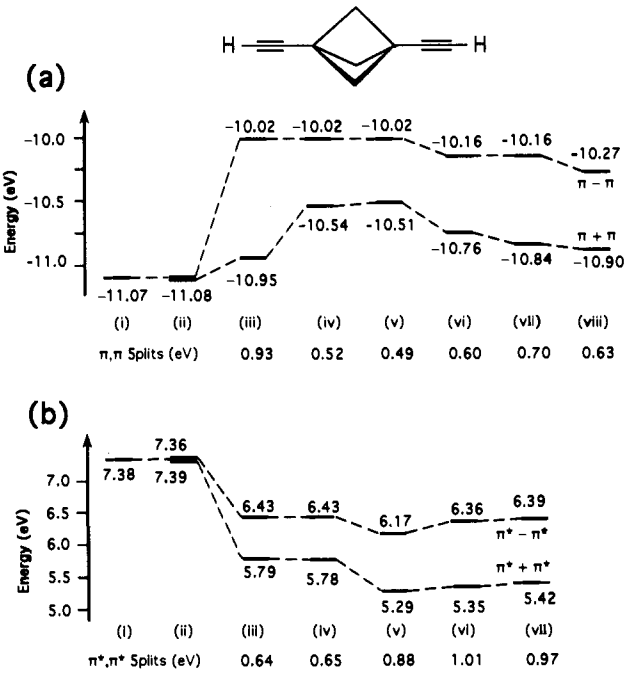

Figure 1. (a) HF/3-21G NBO interaction diagram for the π orbitals in **4(1)**. The interactions are built up in stages, starting with (i) the two degenerate, noninteracting π basis NBO's, and ending with (viii), the energies of the canonical π MO's. The intermediate levels are: (ii) TS mixing between the two π NBO's; (iii) addition of interactions involving the six ring C–C σ NBO's; (iv) addition of interactions involving the six C–H σ NBO's of the CH_2 groups; (v) addition of interactions involving core orbitals; (vi) addition of interactions involving the six ring C–C σ^* NBO's; (vii) addition of interactions involving six C–H σ^* NBO's of the CH_2 groups. (b) HF/3-21G NBO interaction diagram for the π^* orbitals in **4(1)**. The interactions are built up in stages, starting with (i) the two degenerate, noninteracting π^* basis NBO's,[38] and ending with (vii), the energies of the canonical π^* MO's. The intermediate levels are: (ii) TS mixing between the two π^* NBO's; (iii) addition of interactions involving the six ring C–C σ^* NBO's; (iv) addition of interactions involving the six C–H σ^* NBO's of the CH_2 groups; (v) addition of interactions involving "Rydberg" orbitals; (vi) inclusion of interactions involving the six ring C–C and C–H σ NBO's.

The results obtained from application of this procedure to **4(1)** and **4(2)** are summarized in Figures 1 and 2, respectively. From part a of these figures, it is seen that in the π manifold the calculations retaining only the TB coupling involving the C–C σ NBO's give splittings fairly close to those resulting from the full HF calculations (0.93 versus 0.63 eV for **4(1)** and 0.37 versus 0.25 eV for **4(2)**). This is not to say that interactions involving the other NBO's are relatively unimportant, but, rather, that there is a considerable cancellation between the contributions due to the remaining NBO's. For example, in **4(1)** the mixing with the C–H σ NBO's destabilizes the π_+ orbital by 0.41 eV, while the mixing with the C–C σ^* and C–H σ^* NBO's stabilizes it by 0.25 and 0.08 eV, respectively. The net shift in the energy of the π_+ orbital due to interactions involving the C–H σ, C–C σ^*, and C–H σ^* NBO's is thus only 0.08 eV.

One might expect the TB coupling in the π^* manifold to be dominated by mixing with C–C σ^* NBO's. In fact, as can be seen from Figures 1b and 2b, with the 3-21G basis set, the "Rydberg" NBO's associated with the carbon atoms of the bridge also play an important role in the TB coupling in the π^* manifold. For example, for **4(1)** the π_+^*,π_-^* splitting, calculated allowing for all interactions with the C–C σ^* orbitals, is 0.64 eV. When mixing with the "Rydberg" orbitals is included, the π_+^*,π_-^* splitting is 0.88 eV which compares fairly closely with the HF

(35) (a) Heilbronner, E.; Schmelzer, A. *Helv. Chim. Acta* **1975**, *58*, 936. (b) Imamura, A.; Ohsaku, M. *Tetrahedron* **1981**, *37*, 2191. (c) Imamura, A.; Tachibana, A.; Ohsaku, M., *Tetrahedron* **1981**, *37*, 2793. (d) Imamura, A.; Hirao, K. *Tetrahedron* **1979**, *35*, 2243. (e) Ohsaku, M.; Imamura, A.; Hirao, K.; Kawamura, T. *Tetrahedron* **1979**, *35*, 701. (f) Ohsaku, M.; Imamura, A.; Hirao, K. *Bull. Chem. Soc. Jpn.* **1978**, *51*, 3443.

(36) McKinley, A. J.; Ibrahim, P. N.; Balaji, V.; Michl, J. *J. Am. Chem. Soc.* **1992**, *114*, 10631.

(37) In a minimal basis set, the NBO procedure generates sets of occupied and unoccupied valence NBO's as well as core NBO's. With split-valence and larger basis sets, the procedure also generates unoccupied "Rydberg" NBO's.

(38) As pointed out in ref 31b, the energies of the π^* NBO's calculated by the 3-21G basis set are too high, due to the way that the NBO procedure generates the π^* and "Rydberg" NBO's. In this reference it was also noted that more "reasonable" π^* orbital energies can be obtained by allowing for the mixing between the π^* and "Rydberg" NBO's. For the systems of interest here, this requires diagonalization of the 6×6 matrix consisting of the two π^* NBO's and the associated "Rydberg" orbitals. (Six functions are involved because the "Rydberg" orbitals are associated with atoms rather than bonds.)

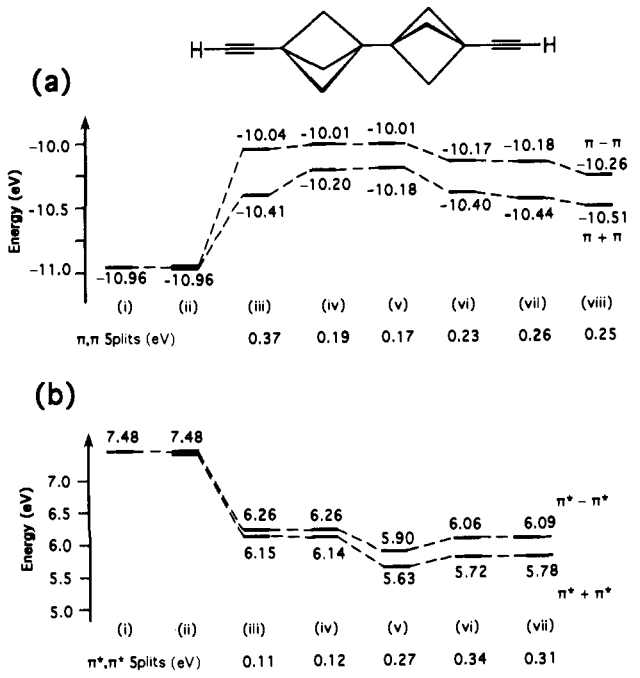

Figure 2. (a) HF/3-21G NBO interaction diagram for the π orbitals in **4(2)**. The interactions are built up in stages, starting with (i) the two degenerate, noninteracting π basis NBO's, and ending with (viii), the energies of the canonical π MO's. The intermediate levels are: (ii) TS mixing between the two π NBO's; (iii) addition of interactions involving the 12 ring C–C σ NBO's; (iv) addition of interactions involving the 12 C–H σ NBO's of the CH_2 groups; (v) addition of interactions involving all core orbitals; (vi) addition of interactions involving the 12 ring C–C σ^* NBO's; (vii) addition of interactions involving 12 C–H σ^* NBO's of the CH_2 groups. (b) HF/3-21G NBO interaction diagram for the π^* orbitals in **4(2)**. The interactions are built up in stages, starting with (i) the two degenerate, noninteracting π^* basis NBO's,[38] and ending with (vii), the energies of the canonical π^* MO's. The intermediate levels are: (ii) TS mixing between the two π^* NBO's; (iii) addition of interactions involving the 12 ring C–C σ^* NBO's; (iv) addition of interactions involving the 12 C–H σ^* NBO's of the CH_2 groups; (v) addition of interactions involving all "Rydberg" orbitals; (vi) addition of interactions involving the 12 ring C–C and C–H σ NBO's.

splitting of 0.97 eV. The mixing with the "Rydberg" orbitals is actually more important (in a relative sense) for **4(2)**, for which the π_+^*,π_-^* splitting, due to mixing with the C–C σ^* NBO's alone, is only 0.11 eV, but increases to 0.27 eV when mixing with the "Rydberg" orbitals is also included. The latter value is in excellent agreement with the HF value of 0.31 eV. Mixing with the C–H σ^* NBO's and with the occupied NBO's (both C–C and C–H) is relatively unimportant for the π_+^*,π_-^* splittings.

Although the NBO analysis described above provides valuable insight into the relative importance of C–C σ, C–H σ, C–C σ^*, C–H σ^*, and "Rydberg" NBO's for TB coupling in the π and π^* manifolds, it still does not permit us to reach conclusions concerning the range of the interactions involved. In order to do this, it is useful to carry out a series of calculations in which interactions retained are selected on the basis of their "range". This approach has recently been used to analyze the TB coupling in a variety of bridge systems.[18,25,30]

We consider first the application of this procedure to the TB coupling in the π manifold. The most important interactions (together with their magnitudes in both the STO-3G and 3-21G basis sets) are shown for **4(2)** in Figure 3. In labeling the interactions, the following scheme has been adopted: each type of interaction is denoted by a letter, with t being reserved for interactions within a staffane unit, S for interactions between adjacent staffane units, and T for interactions coupling the acetylenic π orbitals with the adjacent staffane bridge units. Superscripts are added to indicate the number of bonds skipped,

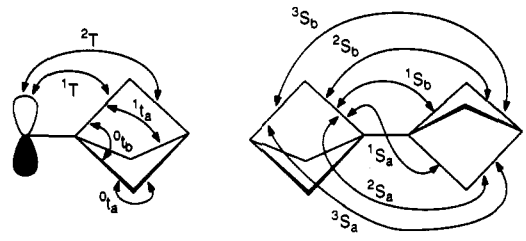

Interactions between occupied NBO's

^1T	1.11 eV (1.21 eV)	^1S_a	0.97 eV (0.98 eV)
^2T	0.27 eV (0.17 eV)	^1S_b	0.24 eV (0.42 eV)
^0t_a	5.23 eV (4.05 eV)	^2S_a	0.44 eV (0.16 eV)
^0t_b	4.23 eV (3.52 eV)	^2S_b	0.16 eV (0.03 eV)
^1t_a	2.15 eV (1.92 eV)	^3S_a	0.00 eV (0.01 eV)
		^3S_b	0.12 eV (0.05 eV)

Interactions between unfilled NBO's

$^1T^*$	2.59 eV (2.32 eV)	$^1S_a^*$	1.87 eV (1.76 eV)
$^2T^*$	0.56 eV (0.31 eV)	$^1S_b^*$	0.97 eV (0.79 eV)
$^0t_a^*$	2.01 eV (2.11 eV)	$^2S_a^*$	0.57 eV (0.24 eV)
$^0t_b^*$	0.82 eV (1.25 eV)	$^2S_b^*$	0.19 eV (0.11 eV)
$^1t_a^*$	0.95 eV (0.95 eV)	$^3S_a^*$	0.06 eV (0.002 eV)
		$^3S_b^*$	0.11 eV (0.03 eV)

Figure 3. Interactions between filled NBO's and between unfilled NBO's in staffanes (the labels for the latter interactions carry an asterisk). The first set of numbers are those obtained with the 3-21G basis set and the second set (in parentheses) were obtained with the STO-3G basis set. The interactions are for **4(2)** at its STO-3G optimized geometry.

and subscripts are used to distinguish nonequivalent interactions involving the same number of skipped bonds. For example, ^0t_a and ^0t_b denote interactions between NBO's associated with adjacent C–C bonds within a staffane unit, and ^1t_a denotes the interaction between two C–C σ NBO's separated by one C–C bond. The various interactions show only a weak sensitivity on environment. For example, the ^0t_a interactions in **4(1)**, **4(2)**, and in the two symmetry inequivalent staffane rings of **4(3)** differ only slightly from one another. These small differences will be ignored in the ensuing discussion.

In the models to be described below, all three types of interactions between the σ NBO's in each staffane ring (i.e., ^0t_a, ^0t_b, and ^1t_a in Figure 3) are included, as are all interactions between the π NBO's and the retained σ NBO's. The most important interactions coupling the π NBO's to the bridges are the ^1T and ^2T interactions, with the former being over four times greater than the latter. Although the inclusion of ^2T interactions is important for obtaining quantitative estimates of the π_+,π_- splittings, it proves to be relatively unimportant for describing the rate of falloff of the splittings with bridge length.

There are six possible interactions between σ NBO's of adjacent staffane rings (viz., two ^1S, two ^2S, and two ^3S). For **4(2)**, the largest matrix elements of each type are 0.97 eV (^1S_a), 0.44 eV (^2S_a), and 0.12 eV (^3S_b), as calculated using the 3-21G basis set. The corresponding values in the STO-3G basis set are 0.98, 0.16, and 0.05 eV. It is clear from these results that interactions other than the short-range ^1S interactions are important for describing the TB coupling between adjacent staffane bridge units.

In order to assess in a more quantitative manner the contributions of the ^3S and ^2S interactions to the TB interactions in the diethynyl[*n*]staffanes, a series of model calculations were performed for **4(1)**–**4(3)**. The four models considered are described below.

Model I: All interactions involving σ^*, core, and "Rydberg" NBO's are deleted.

Table V. π_+,π_- Splitting Energies (eV) and $\beta_h(i,i+1)$ Values (per Bond) Determined from the Splittings for **4(*i*)** and **4(*i*+1)**[a]

	π_+,π_- splitting energies (eV)			$\beta_h(i,i+1)$ (eV)	
approach[b]	**4(1)**	**4(2)**	**4(3)**	$\beta_h(1,2)$	$\beta_h(2,3)$
HF	0.632 (0.523)	0.249 (0.154)	0.111 (0.049)	0.31 (0.41)	0.27 (0.37)
model I	0.515 (0.360)	0.190 (0.085)	0.076 (0.027)	0.33 (0.48)	0.30 (0.38)
model II	0.922 (0.713)	0.374 (0.214)	0.176 (0.075)	0.30 (0.40)	0.25 (0.35)
model III	0.922 (0.713)	0.337 (0.203)	0.142 (0.068)	0.33 (0.42)	0.29 (0.36)
model IV	0.922 (0.713)	0.208 (0.133)	0.049 (0.027)	0.50 (0.56)	0.48 (0.53)

[a] The 3-21G results are given first, followed by the STO-3G results in parentheses. All results in this table are for HF/STO-3G optimized geometries. [b] HF = full SCF values. For explanation of models I–IV, see section IV of the text.

Model II: In addition to those interactions deleted in model I, all interactions with C–H σ NBO's are also deleted.

Model III: In addition to those interactions deleted in model II, ^{3}S interactions are also deleted.

Model IV: In addition to those interactions deleted in model III, ^{2}S interactions are also deleted.

Models I and II were also included in the analysis presented previously, and results for these two models were included in Figures 1a and 2a.

The π_+,π_- splittings and the associated β_h values, obtained from models I–IV and from the full HF calculations, are summarized in Table V. With the 3-21G basis set, model I gives smaller splittings and β_h values about 10% larger than those from the HF calculations. The deviations of the model I results from the HF predictions are due primarily to the deletion of the σ^* and "Rydberg" NBO's rather than to the deletion of the core orbitals. The deletions of the interactions involving the C–H σ NBO's (model II) lead to π_+,π_- splittings about 50% larger than the HF values. In spite of this, the corresponding β_h values are only slightly smaller than the HF values, indicating that comparison of the β_h values from models II–IV should prove adequate for establishing the importance of the ^{1}S, ^{2}S, and ^{3}S interactions for determining the distance dependence of the π_+,π_- splittings.

Comparison of the results of models II and III reveals that deletion of the ^{3}S interactions leads to decreases in the π_+,π_- splittings for **4(2)** and **4(3)** of 5 and 10%, respectively, when using the STO-3G NBO's, and 11 and 20%, when using the 3-21G NBO's. The greater importance of the ^{3}S interactions in the 3-21G basis set is not surprising given the large separation of the bonds involved. In going from model III to model IV, the π_+,π_- splittings of **4(2)** and **4(3)** are found to decrease by about 36 and 63%, respectively, with both the STO-3G and 3-21G basis sets. As a result, the β_h values calculated using model IV are as much as 79% too large. Clearly, inclusion of the ^{2}S interactions is essential for describing the distance dependence of the π_+,π_- splittings.

Even in model IV, in which the coupling between the staffane rings is limited to the relatively short-range ^{1}S interactions, the π_+,π_- splittings are appreciably larger with the 3-21G than with the STO-3G basis set, with the ratio of the 3-21G to STO-3G splittings increasing from 1.29, to 1.56, to 1.81, along the sequence **4(1)**, **4(2)**, and **4(3)**. Thus, even when only ^{1}S interactions between the bridge units are retained, the STO-3G basis set is inadequate for describing the distance dependence of the π_+,π_- splittings. The differences between the ^{1}S interactions in the two basis sets are not large enough to account for these trends; indeed, the ^1S_b interaction, calculated using the STO-3G basis set (0.42 eV), is almost double that calculated using the 3-21G basis set (0.24 eV). Rather, a major factor responsible for this behavior is the larger t-type interactions within individual staffane bridge units as described with the 3-21G basis set.

We now examine briefly the importance of "long-range" ^{2}S* and ^{3}S* interactions for the π_+^*,π_-^* splittings. (The asterisk implies that the interactions are between unoccupied NBO's.) The following three models were considered.

Model I: All interactions involving occupied NBO's are deleted.

Table VI. π_+^*,π_-^* Splitting Energies (eV) and $\beta_e(i,i+1)$ Values (per Bond) Determined from the Splittings for **4(i)** and **4(i+1)**[a]

	π_+^*,π_-^* splitting energies (eV)			$\beta_e(i,i+1)$ (eV)	
approach[b]	**4(1)**	**4(2)**	**4(3)**	$\beta_e(1,2)$	$\beta_e(2,3)$
HF	0.965	0.311	0.104	0.38	0.37
model I	0.872	0.267	0.087	0.39	0.37
model II	0.872	0.195	0.050	0.50	0.45
model III	0.872	0.093	0.022	0.74	0.48

[a] All results in this table are for HF/STO-3G optimized geometries. [b] HF = full SCF values. For explanation of models I–III, see section IV of the text.

Model II: In addition to those interactions deleted in model I, ^{3}S* interactions between adjacent staffane rings are also deleted.

Model III: In addition to those interactions deleted in model II, ^{2}S* interactions between adjacent staffane rings are also deleted.

The π_+^*,π_-^* splittings and associated β_e values for these three models, together with those from the full HF calculations, are summarized in Table VI. Because of the gross inadequacy of the STO-3G basis set for describing the TB coupling between the localized π^* orbitals, only results obtained with the 3-21G basis set are reported.

Model I gives π_+^*,π_-^* splittings only slightly smaller, and β_e values nearly equal to those obtained from the full HF calculations. Omission of the ^{3}S* interactions (model II) leads to 31 and 43% reductions in the values of the π_+^*,π_-^* splittings for **4(2)** and **4(3)**, respectively. The β_e values obtained from model II are over 20% larger than those for model I. Comparison of the results in Tables V and VI shows that the ^{3}S* interactions are more important for the π_+^*,π_-^* splittings than are the ^{3}S interactions for the π_+,π_- splittings.[39]

The π_+^*,π_-^* splittings are smaller still in model III, in which both the ^{2}S* and ^{3}S* interactions are deleted. Moreover, the β_e values obtained with this model imply an even more rapid falloff of the splittings with increasing bridge length than was found in model II.

V. Conclusions

In this work, the π_+,π_- and π_+^*,π_-^* splittings of **4(1)–4(5)** are obtained in the HF approximation, using the STO-3G, 3-21G, and 6-31G* basis sets. For the first three members of the series, calculations have also been performed with several other basis sets. Although the STO-3G basis set suffices for describing qualitatively the trends in the π_+,π_- and π_+^*,π_-^* splittings for the polynorbornyl dienes, **3(2)–3(6)**, this is not the case for the splittings in **4(1)–4(5)**. By means of an NBO analysis it is demonstrated that, as has been shown for a variety of other saturated bridges,[18,25,30] interactions that skip over bonds are very important for describing the coupling between adjacent staffane units. However, a notable difference is that the ^{2}S (and ^{2}S*) interactions, i.e., those that skip over two bonds, are more important in the staffane bridge systems, than in the polynorbornyl dienes **3(2)–3(6)**. This is a major reason why the 3-21G basis

(39) The reason for this can be gleaned from Figure 3, from which it is seen that (with the 3-21G basis set), although the ^1S_b* and ^1S_b interactions are nearly equal, the ^1S_a* interaction is much larger than the ^1S_a interaction.

set is much better than the STO-3G basis set in describing TB interactions in **4(1)**–**4(5)** than in **3(2)**–**3(6)**, whereas in **3(2)**–**3(6)**, the results obtained with these basis sets are qualitatively similar.

The π_+,π_- and the π_+^*,π_-^* splittings of **4(1)**–**4(5)** are found to fall off surprisingly slowly with increasing bridge length, as reflected by the average 3-21G β_h and β_e values of only 0.24 and 0.37 per bond, respectively (see Tables I and II). The distance dependence of the π_+,π_- and the π_+^*,π_-^* splittings for **4(1)**–**4(5)** is even weaker than that calculated for the polynorbornyl dienes, **3(n)**, for which the average 3-21G β_h and β_e values are 0.39 and 0.54 per bond, respectively (Tables III and IV).

Thus, the staffane bridges are predicted to be even more effective than the polynorbornyl bridges at propagating electronic interactions over long distances, *including intramolecular electron transfer and energy transfer processes*.[40] For example, the π_+,π_- and π_+^*,π_-^* splittings in **4(5)** are very close to those of **3(6)**, even though the chromophores are about 6 Å further apart in the former molecule. In comparing the trends in the π_+,π_- (and π_+^*,π_-^*) splittings of the two series, **3(n)** and **4(n)**, it is important to take into consideration the fact that, within the context of the McConnell model (eq 2), the effectiveness of a bridge in propagating interactions depends both on the intrabridge coupling matrix elements, t, and on the energy gap, Δ, separating the chromophore π (π^*) orbitals with the localized bridge σ (σ^*) orbitals. Thus, it is important to note that the π orbital of acetylene is about 1 eV more strongly bound than that of ethylene, leading to smaller σ–π energy gaps in the diethynyl staffane series, **4(n)**, than in the polynorbornyl diene series, **3(n)**. This, in turn, is a major factor responsible for the slower attenuation with increasing bridge length of the π_+,π_- splittings in the staffane series **4(n)**. We anticipate that for the diethenyl staffanes ([**n**]**1**; X and Y = $-CH{=}CH_2$) the π_+,π_- splittings should fall off more rapidly with the number of bridge units than in the diethynyl staffanes studied here. This point is currently under investigation.

For **4(1)** the π_+^*,π_-^* splitting is larger than the π_+,π_- splitting. However, for **4(5)** the π_+,π_- splitting is about four times larger than the π_+^*,π_-^* splitting, due to the more rapid falloff of the π_+^*,π_-^* splittings with bridge length. Examination of the matrix elements between individual unoccupied NBOs (Figure 3) reveals that the $^1T^*$, $^2T^*$, $^1S^*$, and $^2S^*$ interactions are all significantly larger than the corresponding couplings between the filled NBO's. Based on these observations, one would expect the π_+^*,π_-^* splittings to be larger and to fall off more slowly with bridge length than the corresponding π_+,π_- splittings. That this is not the case is due to the fact that the t matrix elements are much larger than the t* matrix elements. Thus, the more rapid attenuation of the π_+^*,π_-^* splittings, compared the π_+,π_- splittings in **4(1)**–**4(5)** with increasing bridge length is actually due to the fact that the couplings between the σ^* NBO's are smaller than those between σ NBOs within the individual staffane rings.

Acknowledgment. We are grateful to the Australian Research Council (M.N.P.-R.) and the National Science Foundation (K.D.J.) for continuing support. We also thank Mr. Stephen S. Wong for carrying out preliminary geometry optimizations on **4(1)** and Dr. Marshall D. Newton for helpful advice and encouragement.

(40) This prediction may need qualification when applied to bichromophoric staffanes, [n]**1**, in which the two chromophores, X and Y, are conformationally mobile with respect to their rotation about the major axis of the staffane. This situation obtains for chromophores that are not cylindrically symmetric with respect to the staffane major axis, such as vinyl groups, quinones, etc. In these cases, the strength of the TB coupling between the chromophores depends sensitively on their orientation with respect to each other, as well as their separation.